npg

Original Article

Ric-3 chaperone-mediated stable cell-surface expression of the neuronal α7 nicotinic acetylcholine receptor in mammalian cells

Ana Sofía VALLÉS, Ana M ROCCAMO, Francisco J BARRANTES*

Instituto de Investigaciones Bioquímicas de Bahía Blanca and UNESCO Chair of Biophysics and Molecular Neurobiology, CC 857, B8000FWB, Bahía Blanca, Argentina

Aim: Studies of the α7-type neuronal nicotinic acetylcholine receptor (AChR), one of the receptor forms involved in many physiologically relevant processes in the central nervous system, have been hampered by the inability of this homomeric protein to assemble in most heterologous expression systems. In a recent study, it was shown that the chaperone Ric-3 is necessary for the maturation and functional expression of α7-type AChRs[1]. The current work aims at obtaining and characterizing a cell line with high functional expression of the human α7 AChR.
Methods: Ric-3 cDNA was incorporated into SHE-P1-hα7 cells expressing the α7-type AChR. Functional studies were undertaken using single-channel patch-clamp recordings. Equilibrium and kinetic [125I]α-bungarotoxin binding assays, as well as fluorescence microscopy using fluorescent α-bungarotoxin, anti-α7 antibody, and GFP-α7 were performed on the new clone.
Results: The human α7-type AChR was stably expressed in a new cell line, which we coined SHE-P1-hα7-Ric-3, by co-expression of the chaperone Ric-3. Cell-surface AChRs exhibited [125I]αBTX saturable binding with an apparent K_D of about 55 nmol/L. Fluorescence microscopy revealed dispersed and micro-clustered AChR aggregates at the surface of SHE-P1-hα7-Ric-3 cells. Larger micron-sized clusters were observed in the absence of receptor-clustering proteins or upon aggregation with anti-α7 antibodies. In contrast, chaperone-less SHE-P1-hα7 cells expressed only intracellular α7 AChRs and failed to produce detectable single-channel currents.
Conclusion: The production of a stable and functional cell line of neuroepithelial lineage with robust cell-surface expression of neuronal α7-type AChR, as reported here, constitutes an important advance in the study of homomeric receptors in mammalian cells.

Introduction

Nicotinic acetylcholine receptors (AChRs) participate in many cellular and physiological processes. They are members of the Cys-loop family of neurotransmitter-gated ion channels, all of which are pentameric transmembrane receptors[2]. AChRs are expressed in both the central and peripheral nervous systems (the neuromuscular junction and the electromotor synapse of electric fish). The homomeric α7 AChR is one of the most abundant AChR subtypes in the mammalian central nervous system[3]. Of the entire central nervous system, it is the hippocampus — the area of the brain involved in various aspects of learning and memory — that exhibits the highest levels of α7 AChR protein. The α7 AChR can act presynaptically, postsynaptically and peri-synaptically to facilitate the liberation of neurotransmitters, mediate synaptic transmission[4] or modulate connections with different neurons by activating diverse second messenger routes. It is believed that these functions are carried out largely as a consequence of their high permeability to calcium[5], since the entry of Ca^{2+} facilitates the liberation of neurotransmitters.

The α7 AChRs are related to various diseases such as Alzheimer's, schizophrenia, certain types of epilepsy and Parkinson's disease[6]. Complete characterization of the kinetic and pharmacological properties of α7 AChRs is key both to

understanding the physiopathological mechanisms operating in these diseases and to opening new avenues for developing therapeutic intervention.

The α7 AChR has proved very difficult to express in mammalian cells. Although there have been reports on the expression of α7 AChR in various of these cells[7, 8], functional receptors have been very hard to obtain in practically all the cell lines studied to date[9–12]. Previous reports indicated that the Ric-3 protein is necessary to produce detectable levels of α7 AChRs at the cell surface. Ric-3, first discovered in *Caenorhabditis elegans*, is an endoplasmic reticulum–resident protein present in cells that endogenously express α7 AChR[13]. Ric-3 has been shown to increase α7 AChR heterologous expression in oocytes from *Xenopus laevis* and in mammalian cell lines such as HEK-293[13–17]. According to these authors, Ric-3 is needed to attain the correct folding of the α7 AChR, and therefore to attain functional expression. Furthermore, William *et al*[13] contend that Ric-3 does not increase the transport of α7 AChR from the ER to the cell surface membrane; rather, it facilitates the correct assembly at the ER, thereby increasing the expression of functional cell-surface AChRs. They further argue that in the absence of Ric-3, palmitoylation of α7 AChRs would not occur, thus preventing functional heterologous expression of these receptors in HEK-293 cells. It is worth mentioning that other proteins are also palmitoylated in this type of cell. In 2004, Drisdel *et al*[15] proposed that the role of Ric-3 fits the definition of a specific chaperone that renders cysteine residues of α7 subunits accessible to palmitoylation in the ER, since cells that do express functional α7 AChR in their plasma membrane, such as PC12 cells and oocytes, express Ric-3 endogenously[13, 15]. Most studies indicate that Ric-3 does not remain associated with assembled AChRs at the cell surface[1]. The low levels of cell-surface expression have limited our understanding of the kinetic activation of α7 AChRs. Few studies have reported single-channel currents in oocytes from wild-type and mutant α7 AChRs[18, 19]. Recently, the human α7 AChR and the Ric-3 protein were transiently transfected in BOSC 23 cells[20]. Furthermore, Roncarati *et al*[21] produced a CHO-derived cell line that stably expresses α7 AChRs with the aid of the Ric-3 chaperone.

Although the neuroepithelial cell line SHE-P1-hα7 expresses α7 AChRs in a stable manner[8], the levels of surface expression are so low that the receptor protein cannot be detected by conventional fluorescence microscopy or electrophysiological techniques. In the present report, SHE-P1-hα7 cells are shown to display robust α7 AChR expression at the cell membrane upon transient transfection with Ric-3 cDNA. In addition, a novel cell line was obtained (SHE-P1-hα7-Ric-3) that stably expresses functional α7 AChRs at the cell surface by co-transfection of the Ric-3 protein, thus opening new possibilities for characterizing the α7 AChR in mammalian cells.

Materials and methods

Cell culture, plasmid construction and production of the novel cell line SHE-P1-hα7 cells[22] were cultured in DMEM supplemented with 5% fetal bovine serum, 10% horse serum and Hygromycin B in a Napco 6100 incubator at 37 °C with 5% CO_2. The new clone, SHE-P1-hα7-Ric-3, was obtained by transfection of Ric-3 cDNA (kindly provided by Prof M CRIADO, Instituto de Neurociencias de Alicante, Universidad Miguel Hernández, Alicante, Spain) into SHE-P1-hα7 cells[22] using FuGENE 6 (Roche, Indianapolis). Selection of positive clones was performed 48 h later by incubating the cells with G418 (400 mg/L). Every two days the cell culture medium was changed to remove dead cells. A novel cell line was produced that expressed both α7 AChR and the Ric-3 protein in a stable manner. SHE-P1-hα7-Ric-3 cells were subsequently cultured in DMEM supplemented with G418 (40 mg/L) and Hygromycin B with 5% fetal bovine serum, 10% horse serum and Hygromycin B as above. GFP-α7 was constructed by subcloning into the *Sal*/*Bam*HI sites of pEGFP-N2 (Clontech, Palo Alto, CA) in Prof Criado's laboratory (Instituto de Neurociencias de Alicante, Universidad Miguel Hernández, Alicante, Spain). Ric-3 cDNA was subcloned into the *Xho*I/*Eco*RI sites of pEGFP-N1 (Clontech, Palo Alto, CA) at the Instituto de Neurociencias in Alicante.

Patch-Clamp recordings Single-channel currents were recorded in the cell-attached configuration at membrane potentials of -70, +50, and +70 mV at 20 °C using an Axopatch 200B patch-clamp amplifier (Axon Instruments, Inc, CA), digitized at 94 kHz with an ITC-16 interface (Instrutech Corporation, Long Island, NY) and transferred to a computer using Acquire software (Bruxton Corporation, Seattle, WA). The bath and pipette solutions contained 142 mmol/L KCl, 5.4 mmol/L NaCl, 1.8 mol/L $CaCl_2$, 1.7 mmol/L $MgCl_2$ and 10 mmol/L HEPES (pH 7.4). Patch pipettes were pulled from Kimax-51 capillary tubes (Kimble Products, Vineland, NJ), coated with Coat D (M-Line accessories, Measurements Group, Raleigh, NC), and fire-polished. Pipette resistances ranged from 5 to 7 MΩ. ACh working solutions (50 µmol/L) were dissolved in the bath solution and applied to the cell through the patch pipette tip. Detection of single-channel events using the program TAC followed the half-amplitude threshold criterion (Bruxton

Corporation, Seattle, WA) at a bandwidth of 5 kHz. The sampling time was 20 μs and the minimum detectable interval was 0.066 ms. Open, burst and closed-time histograms were plotted using a logarithmic abscissa and a square root ordinate. They were then fitted to the sum of exponential functions by the maximum likelihood criterion using the TACFit program (Bruxton Corporation, Seattle, WA). Burst resolution was obtained from the intersection between the main closed-time component and the succeeding one.

Fluorescence microscopy Cells were grown on 25 mm diameter glass coverslips in DMEM for 2–3 days at 37 °C. Cells were washed twice with M1 buffer (150 mmol/L NaCl, 1 mmol/L CaCl$_2$, 1 mmol/L MgCl$_2$, and 5 mmol/L KCl in 20 mmol/L HEPES buffer, pH 7.4). Cell-surface AChR labeling was carried out by incubating the cells with Alexa^{488}αBTX, Alexa^{594}αBTX, or Alexa^{555}αBTX at a final concentration of 1 μmol/L (15 min, 4 °C) or with anti-α7 AChR monoclonal antibody (H-302, Santa Cruz Biotechnologies, Santa Cruz, CA, 1 h at 4 °C) followed by Alexa^{555}goat anti-rabbit secondary antibody (1 h, 4 °C). Cells were subsequently rinsed three times with M1 and mounted for microscope examination. For intracellular α7 AChR labeling, cells were fixed with 2% paraformaldehyde for 10 min and then permeabilized with 0.01% Triton X-100 for an additional 10 min. Finally, cells were incubated for 15 min with Alexa^{488}αBTX. As a negative control for fluorescent microscopy, cells were incubated in the presence of Alexa^{555}goat anti-rabbit secondary antibody (1 h, 4 °C), washed three times with M1 and mounted for microscope examination. No fluorescence was observed after this treatment.

Overexpression of GFP-α7 in SHE-P1-hα7 cells was carried out using Lipofectamine 24 h after cell plating following the protocol provided by the manufacturer (Gibco BRL, Life Technologies, Buenos Aires). Cells were visualized 48 h later.

Wide-field fluorescence microscopy Imaging was carried out using a Nikon Eclipse E-600 microscope equipped with 40X NA 1.0 or 100X NA 1.4 objectives, digitized with a model ST-7 SBIG digital charge-coupled device camera (765×510 pixel, 9.0×9.0 mm pixel size; Santa Barbara, CA), and thermostatically cooled at -10 °C. The ST-7 CCD camera was driven by the CCDOPS software package (SBIG Astronomical Instruments, version 5.02). Appropriate excitation, dichroic and emission filters were employed to avoid crossover of fluorescence emission following previously established conditions[32, 33]. Sixteen-bit TIFF images were exported for further offline analysis.

Confocal microscopy Images were obtained with a TCS-SP2 confocal microscope (Leica Mikrosysteme Vertrieb GmbH, Wetzlar, Germany) equipped with an acousto-optical beam splitter. Fluorescence images were analyzed with Scion Image software, version 4.0.2 (Scion Corporation, Frederic, MD).

Equilibrium and kinetic [^{125}I]αBTX binding studies Surface AChR expression was determined by incubating 70–80% confluent cells with increasing concentrations (0.01–150 nmol/L) of [^{125}I]αBTX in cell culture medium for 15 min at 25 °C. At the end of the incubation period, dishes were washed twice with high-potassium Ringer's solution, then cells were removed by scraping, and collected with 0.1 Eq/L NaOH. Non-specific binding was determined from the radioactivity remaining in the dishes after the initial preincubation of the cells in 10 μmol/L native αBTX or 100 mmol/L carbamoylcholine chloride before addition of [^{125}I]αBTX. Total AChR was determined after lysis of the cells. Briefly, cells were lysed for 5 min at 25 °C in buffer containing 1% saponin and the binding assay was carried out as described above. Non-specific binding accounted for approximately 10%–30% of the total binding. Radioactivity was measured in a gamma counter with an efficiency of 80%. The metabolic half-life of surface AChRs was determined by labeling cell cultures with 40 nmol/L [^{125}I]αBTX for 15 min at 25 °C, washing twice and incubating for the indicated periods. For the equilibrium experiments, non-specific binding was determined as described above. The half-time of degradation was determined from nonlinear regression analysis of the decay curve corresponding to the radioactivity retained by the cells at different intervals. This followed a monoexponential time-course. The K_D was calculated from linear regression analysis of the kinetics of [^{125}I]αBTX association.

Inhibition of the initial rates of αBTX binding Cells were resuspended in high-potassium Ringer's solution and pre-incubated for 10 min in the absence or presence of nicotine. [^{125}I]αBTX was added to a final concentration of 40 nmol/L for an additional 15 min. Binding was stopped by centrifugation for 5 min at 2000×g. Each experiment was carried out twice in triplicate, and results were analyzed by normalizing to the binding in the absence of any competitive ligand. Radioactivity was measured in a gamma counter with an efficiency of 80%. The K_i value for nicotine was calculated from the concentration-dependent inhibition using the equation $K_i = IC_{50}/1 + [[^{125}I] \, αBTX/K_D]$[23]

Data analysis Data are expressed as mean±SD from independent experiments. Statistical analysis was performed using Student's *t*-test. A value of $P \leqslant 0.05$ was considered statistically significant.

Results

Native α7 AChR expression in SHE-P1-hα7 cells The human epithelial cell line SHE-P1[24] shares a common neuroepithelial ancestry with neurons. SHE-P1 cells that stably express human α7 AChRs (SHE-P1-hα7) but lack other subtypes of nicotinic receptors have been produced, and some of the pharmacological properties of this cell line have been characterized[8]. The mRNA products of SHE-P1-null (the parental cell line) and SHE-P1-hα7 cells after RT-PCR are shown in Supplementary Figure 1; only SHE-P1-hα7 cells express mRNA for the α7 subunit. In accordance with previous observations, α7 AChR protein expression is restricted to the intracellular compartment, despite the presence of α7 mRNA elsewhere (Figure 1B). Confocal microscopy of intact, non-permeabilized SHE-P1-hα7 cells stained with Alexa[488]αBTX revealed that the protein is absent from the cell (Figure 1A).

In order to estimate the level of α7 AChR expression, radioligand binding studies were carried out in parallel using [125I]αBTX. Figure 1C compares the levels of total and cell-surface pools of [125I]αBTX binding sites in SHE-P1-hα7 cells. Less than 1% of the total α7 AChRs is expressed at the cell surface in SHE-P1-hα7 under normal conditions (Figure
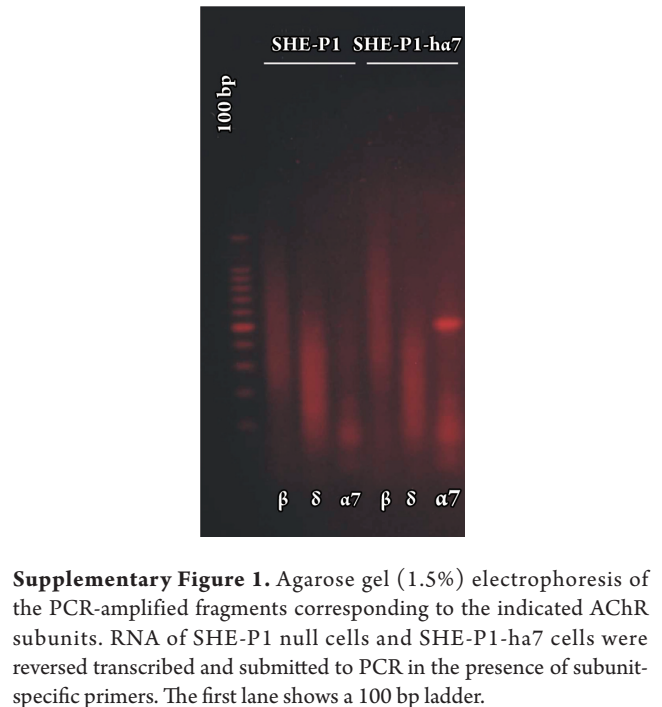
Supplementary Figure 1. Agarose gel (1.5%) electrophoresis of the PCR-amplified fragments corresponding to the indicated AChR subunits. RNA of SHE-P1 null cells and SHE-P1-ha7 cells were reversed transcribed and submitted to PCR in the presence of subunit-specific primers. The first lane shows a 100 bp ladder.

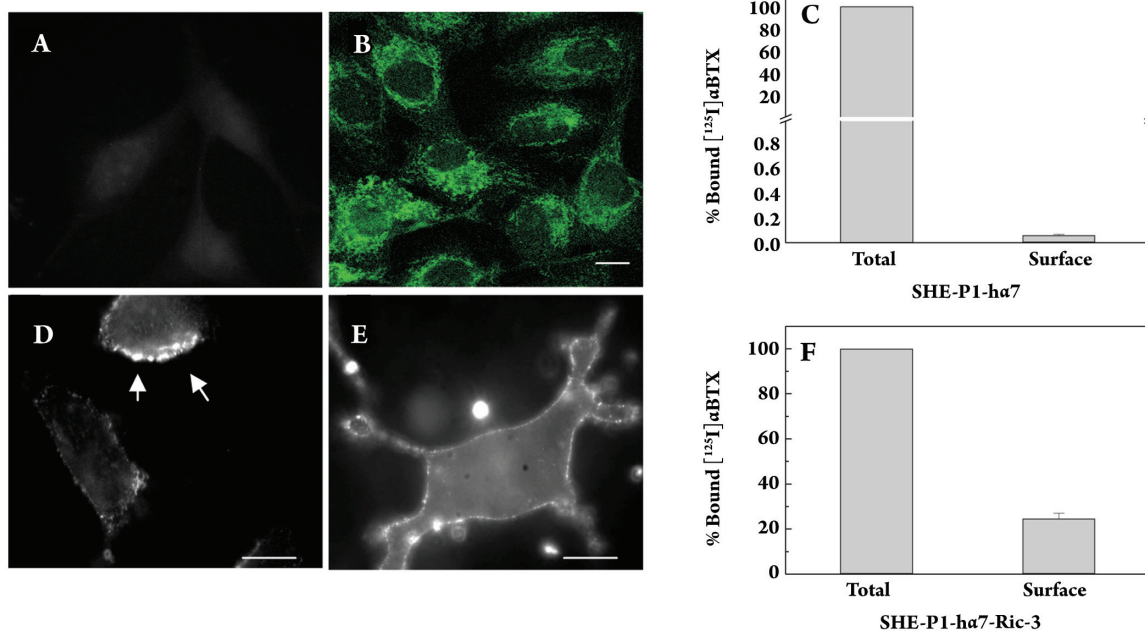1C).

Next, we sought to enhance the level of α7 AChR expres-

Figure 1. Basal α7-AChR expression in SHE-P1-hα7 cells and enhanced stable cell-surface expression of human α7-type AChR in the new clonal cell line, SHE-P1-hα7-Ric-3. Confocal images of A) cell-surface (Alexa[488]αBTX) and B) intracellular Alexa[488]αBTX staining of SHE-P1-hα7 cells. C) Histogram depicting the proportion of total and cell-surface pools of [125I]αBTX binding sites in SHE-P1-hα7 cells. Wide-field fluorescence microscopy of D) cell-surface (Alexa[594]αBTX) and E) anti-α7 AChR staining. F) Histogram showing the proportion of total and cell-surface pools of [125I]αBTX binding sites in SHE-P1-hα7-Ric-3 cells. Scale bar=20 μm (×1000).

sion at the cell surface. In an initial series of experiments, cells were re-transfected with α7 subunit cDNA and incubated for 48 h in the presence of nicotine or at a lower temperature (25 °C, as in ref [22] for the same period). The level of expression of α7 AChRs at the cell surface of SHE-P1-hα7 could still not be detected by conventional wide-field fluorescence microscopy or by electrophysiological techniques at the single-channel level (data not shown), indicating that enhancing the levels of plasmid DNA is not sufficient to increase cell-surface expression.

Heterologous expression of Ric-3 establishes a robust cell-surface expression of α7 AChR Given the successful use of the chaperone protein Ric-3 on α7 AChR expression in heterologous systems[1], SHE-P1-hα7 cells were transiently transfected with human Ric-3 (see Materials and methods) and α7 AChR expression was evaluated by fluorescent αBTX binding (Supplementary Figure 2). It became apparent that α7 AChR cell-surface expression increased remarkably upon co-expression of Ric-3 when compared with that of SHE-P1-hα7 cells not transfected with the chaperone protein.

This finding led us to attempt to express both proteins, Ric-3 and α7 AChR, in a stable manner. For this purpose, SHE-P1-hα7 cells with a constitutively expressed α7 gene (Hygromycin B selection) were transfected with human Ric-3, and maintained in culture with G418 selection medium (see Materials and methods). Positive clones were subsequently selected. Cell-surface expression in one such clone, coined SHE-P1-hα7-Ric-3, was assessed by αBTX binding using Alexa594αBTX or anti-α7 monoclonal antibodies. The surface pool of α7 AChRs in intact, living SHE-
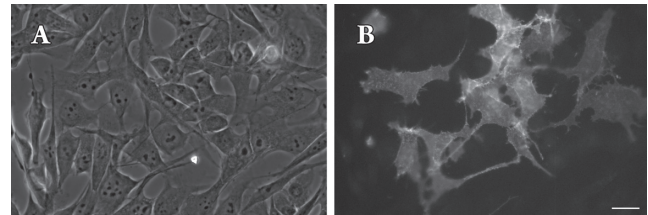
Supplementary Figure 2. Transient overexpression of α7 AChR in SHE-P1-hα7 cells. Cells were transfected with the Ric-3 chaperone cDNA 48 h before fluorescence microscopy as described in Material and Methods. (a) Phase contrast image of SHE-P1-hα7 cells and (b) Alexa488αBTX staining for 15 min at 4 °C and imaged with 40×magnification in a Nikon E-300 inverted epifluorescence microscope. Scale bar=20 μm (×400).

P1-hα7-Ric-3 cells displayed a finely punctate distribution all along the cell surface when stained with Alexa594αBTX (Figure 1D) or anti-α7 monoclonal antibodies followed by the Alexa594 secondary antibody (Figure 1E). "Hot spots" were also observed (arrows) with the monovalent ligand (the fluorescent αBTX). It should be noted that cells were examined 15 min after exposure to [125I]αBTX or Alexa-labeled αBTXs. This relatively brief incubation with the toxin was chosen after determining the optimal AChR rendering at the plasmalemma (5–120 min). Longer periods of incubation (>15 min) already showed a considerable degree of AChR internalization (Supplementary Figure 3). The results of the fluorescence microscopy experiments were corroborated by [125I]αBTX binding and the number of [125I]αBTX binding sites was found to increase by about 20% when Ric-3 was sta-

15 min	30 min	1 h	2 h
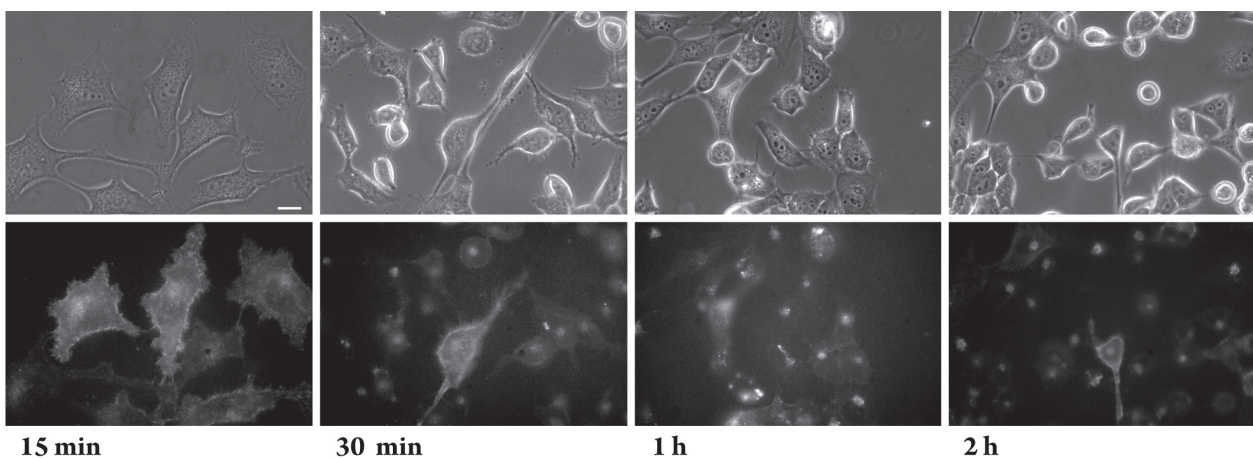
Supplementary Figure 3. Optimization of μ7 AChR fluorescent α-bungarotoxin staining of SHE-P1-hα7-Ric-3 cells. The rapid nternalization of the AChR in the clonal cell line called for shorter times of the fluorescence staining protocol. The upper row shows phase contrast images of SHE-P1-hα7-Ric-3 cells and the lower row shows the corresponding fluorescence (Alexa488αBTX) cell-surface staining of α7AChR at the indicated times. All subsequent cell-surface staining was carried out for 15 min only. Scale bar=20 μm (×400).

bly expressed (Figure 1F).

The enhanced expression was restricted to the transiently expressed GFP-α7 . Figure 2 shows wide-field microscopy images of these cells 48 h after transfection. GFP-α7 was also found at the cell membrane, co-localizing with Alexa[555]αBTX staining. Interestingly, in addition to the predominantly finely punctate and spotty distribution observed with fluorescent bungarotoxin-stained α7 AChRs at the cell surface (single arrows, red staining), larger aggregates of GFP-labeled α7 AChRs (green) were observed (Figure 2, circles) that co-localized (Figure 2, merge) with larger clusters of presumably constitutively expressed AChRs tagged with Alexa[555]αBTX. Another form of cell-surface receptor aggregates was also observed in ~55% of the cells: several micron-sized "patches" (bracket) reminiscent of the large AChR clusters in developing myotubes[25].
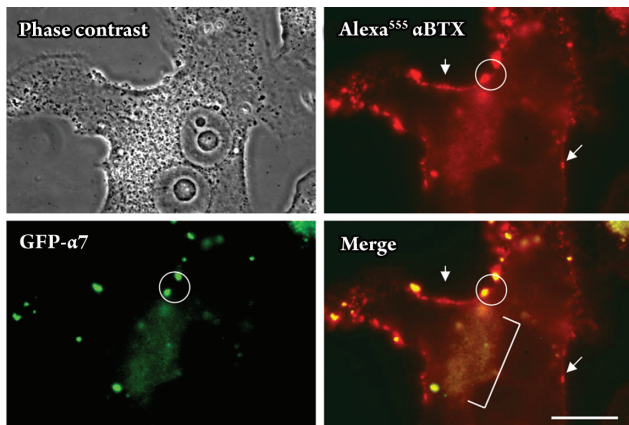

Figure 2. Transient cell-surface expression of GFP-α7 in SHE-P1-hα7-Ric-3. Wide-field fluorescence microscopy of α7 AChR in SHE-P1-hα7-Ric-3 cells 48 h after transfection with GFP-α7. Constitutively expressed AChR predominantly shows a finely punctuate, spotty distribution at the cell surface (stained red with Alexa[555]αBTX) and larger clusters (single arrows) that co-localize (merged image) with the larger clusters of transiently expressed GFP-labeled AChR (green). Micron-sized patches (double arrows) are also apparent. Scale bar=30 μm (×1000).

Equilibrium binding and kinetics of [125I]αBTX to SHE-P1-hα7-Ric-3 cells Next, we investigated the kinetics and equilibrium binding of [125I]αBTX in SHE-P1-hα7-Ric-3 cells (Figure 3). Cells were incubated for 15 min with increasing concentrations of [125I]αBTX (Figure 3A). B_{max}, the maximum number of binding sites, was estimated to be 233.2 fmol/mg protein and the apparent equilibrium binding constant, K_D, 54.92±9.2 nmol/L (Figure 3B).

Studies of the association kinetics of [125I]αBTX to the α7 AChR yielded a half-time of about 7.0 min (Figure 3C). Linearization of the kinetic curves, obtained by plotting ln (Beq/Beq - Bt) as a function of time[26], yielded an apparent k_{on} value of 32.3±1.32 h^{-1}. The half-time for dissociation was calculated to be 20.0 min (Figure 3D).

Pharmacological properties of the α7 AChR in SHE-P1-hα7-Ric-3 cells Studies were conducted next to evaluate the pharmacological properties of the α7 AChR in SHE-P1-hα7-Ric-3 cells. To this end, we incubated the cells with increasing concentrations of nicotine for 10 min at room temperature prior to the application of 40 nmol/L [125I]αBTX for an additional 15 min at 4 °C. As evidenced by the data presented in Figure 3E, nicotine competes with αBTX for the agonist/antagonist binding site. The calculated IC$_{50}$ for nicotine was about 40 μmol/L and the K_i value was 23.26 μmol/L.

Functional properties of α7 AChR in SHE-P1-hα7-Ric-3 cells The functional properties of the α7 AChR expressed in SHE-P1-hα7-Ric-3 cells were studied using the patch-clamp technique. Single-channel currents were recorded from cells exposed to 50 μmol/L ACh at different membrane potentials (Figure 4A). The α7 AChR exhibited two main open-time durations at -70 mV, τ_{open1}=0.29±0.1 ms and τ_{open2}=0.67±0.03 ms, the former being the predominant component. At +50 mV, τ_{open1} lasted 0.12±0.02 ms and τ_{open2}=0.42±0.07 ms; their relative weight was about the same. Open-time durations at different membrane potentials are shown in Figure 4B.

Closed-time intervals exhibited two main components at positive potentials (Figure 4C). The first, τ_{close1}, most likely represents the transition of a channel that opens, closes and reopens. The second component, τ_{close2}, represents intervals between individual openings of a single channel. At negative membrane potentials, three closed-time components were observed. The third component possibly represents transitions to a desensitized AChR, which becomes more evident at negative membrane potentials (Figure 4C).

Two burst-time components were identified at all membrane potentials assayed (Figure 4D). At +50 mV and -70 mV, the first component lasted 0.29±0.15 ms and 0.26±0.13 ms, respectively, probably reflecting unitary apertures. The second component lasted 1.28±0.82 ms and 0.90±0.33 ms, respectively, indicating that some openings occurred in groups at 50 μmol/L ACh.

Finally, we evaluated the amplitudes of the currents generated by channel openings (Figure 4E). Histograms obtained at different membrane potentials revealed that there were two to three different levels of channel amplitudes (Amp$_1$=6.92±2.86 pA, Amp$_2$=12.53±1.43 pA, at -70 mV).
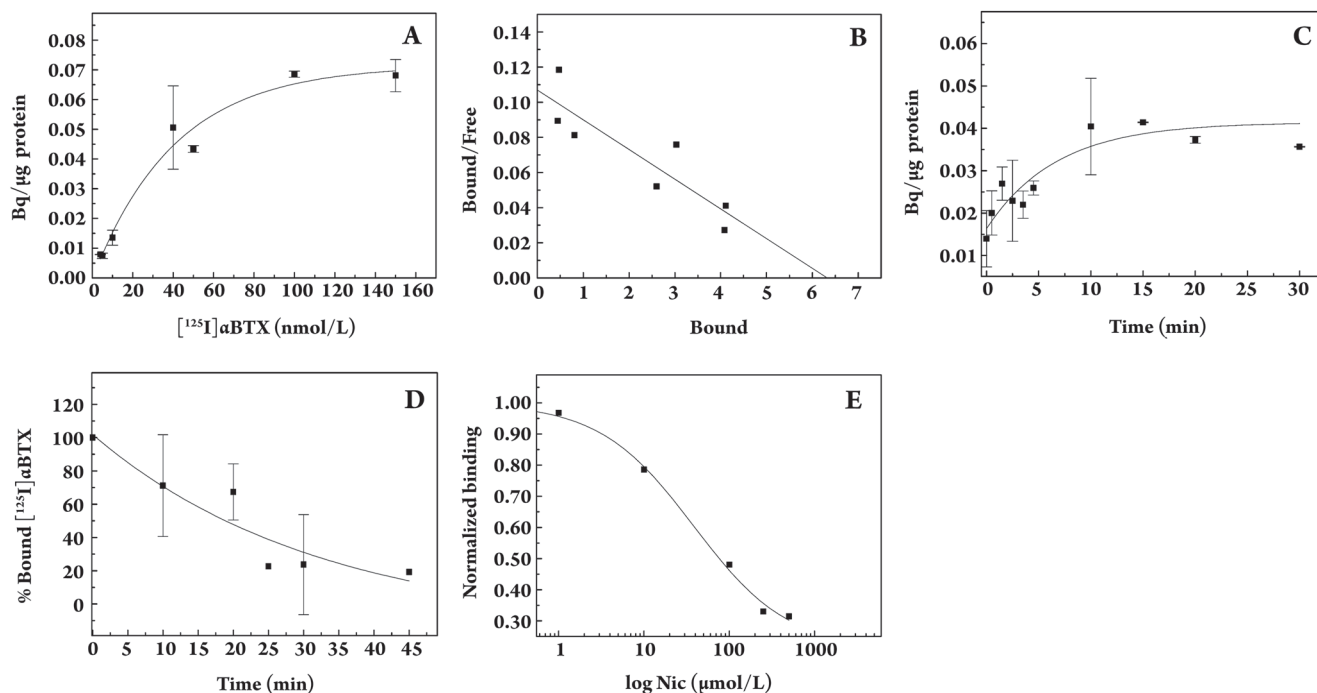
Figure 3. Equilibrium binding of $[^{125}I]\alpha BTX$ to SHE-P1-hα7-Ric-3 cells. A) Cells were incubated with $[^{125}I]\alpha BTX$ for 15 min at the indicated concentrations. B) Scatchard plot corresponding to the data shown in (A). B_{max}, the maximum number of binding sites, was estimated to be 233.19 fmol/mg protein and the K_D=54.92 nmol/L. (C) Radiolabeled toxin association kinetics. Cells were incubated for the indicated times with 40 nmol/L $[^{125}I]\alpha BTX$. Half-time was reached at about 7.0 min. (D) Cells were incubated with 40 nmol/L $[^{125}I]\alpha BTX$ for 15 min, washed thrice and samples collected for radioactivity measurements at the indicated times, yielding a $t_{1/2}$ about 20 min. Data are mean values±SD of at least three different samples. E) Inhibition by nicotine of the initial rate of $[^{125}I]\alpha BTX$ binding to SHE-P1-hα7-Ric-3 cells. Cells were incubated with the indicated concentrations of nicotine at RT for 10 min. $[^{125}I]\alpha BTX$ (40 nmol/L) was then added for an additional 15 min at 4 °C. The calculated IC_{50} is about 40 μmol/L.

Discussion

The neuronal α7 is the only mammalian subunit that appears to preferentially form homomeric, rather than heteromeric, receptors in heterologous expression systems[27–29]. Although α7 subunits form functional homomeric AChRs when expressed in *Xenopus* oocytes, they do so much less efficiently in many types of cultured cell lines[10–12, 30].

In comparison with several other transmembrane proteins, the assembly of ion channels, such as the AChR, is a slow and inefficient process. Each subunit must adopt the correct transmembrane topology and undergo critical post-translational modifications[31]. Proper conformational folding of the subunit is essential for the formation of fully assembled pentameric receptors. The early steps of receptor folding and assembly occur within the ER, the intracellular compartment containing several proteins required for efficient protein folding and post-translational modification[31]. There is evidence that AChR folding, assembly and trafficking are influenced by several chaperone proteins. Recent studies have shown that co-expression of α7 AChR and the chaperone RIC-3 facilitates the formation of functional homomeric AChRs in otherwise non-permissive cell types[13, 14, 16, 17]. RIC-3 was originally identified in the nematode *Caenorhabditis elegans as* a protein encoded by the gene *ric*-3 (resistance to inhibitors of cholinesterase) and has subsequently been cloned and characterized for mammalian and insect species. RIC-3 is required for efficient folding, assembly and functional expression of receptors and, unlike other chaperone proteins, appears to be highly specific in its chaperone activity. RIC-3 is a transmembrane ER-resident protein, with most studies indicating that it does not remain associated with assembled AChRs at the cell surface[1].

In this work, stable expression of the Ric-3 protein in SHE-P1-hα7 cells led to the production of a new cell line, SHE-P1-hα7-Ric-3, which exhibits robust α7 subunit cell-surface expression. The levels of cell-surface α7 AChRs in this new cell line increased from less than 1% to 20% (Figure
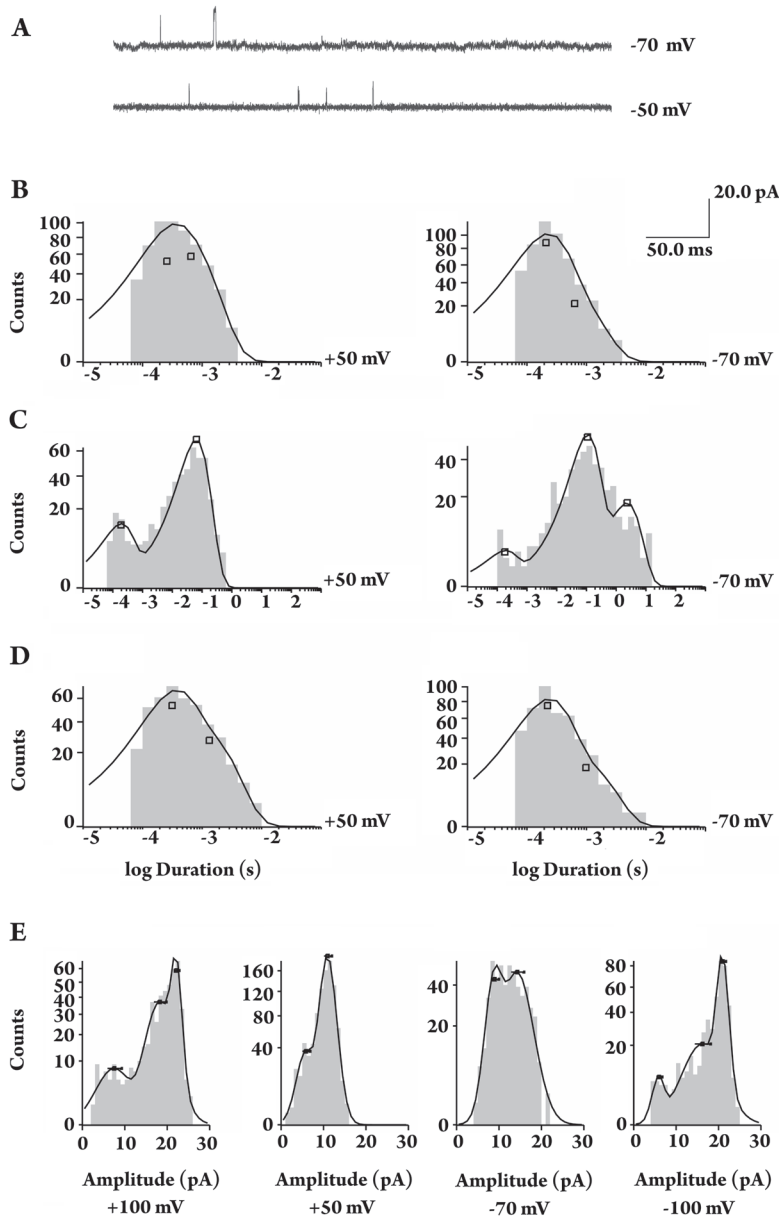
Figure 4. Single-channel patch-clamp recordings of ACh-activated channels in SHE-P1-hα7-Ric-3 cells. A) Raw traces of single-channel currents (50 μmol/L ACh). B) Open-time histograms of α7 AChRs at two different membrane potentials (+50 mV, left; -70 mV, right). C) Closed-time histograms of α7 AChRs expressed in SHE-P1-hα7-Ric-3 cells, at two different membrane potentials (+50 mV, left; -70 mV, right). D) Burst-time histograms at +50 mV (left) and -70 mV (right). E) Amplitude histograms at the indicated membrane potentials.

1). On the basis of previous reports[13, 14, 16, 17], we can surmise that Ric-3 facilitates the correct folding and assembly of α7 subunits at the ER. When the parental SHE-P1-hα7 cells were labeled with fluorescent αBTX, a punctate distribution reminiscent of the ER staining was observed throughout the cell (Figure 1B). This localization of the receptor proteins is highly suggestive of retention and accumulation of unassembled receptors in the ER, as previously observed with *Torpedo* muscle AChRs expressed in mouse fibroblasts[31] or with adult muscle AChRs in CHO cells[32].

The association kinetics of αBTX to α7 AChRs in SHE-P1-hα7-Ric-3 cells is much faster (apparent k_{on}=32.3±1.32

h^{-1}) than for adult muscle-type AChRs expressed in CHO-K1/A5 cells[33] (k_{on}=1.2±0.12 h^{-1}). The half-life of the α7 AChRs was also much shorter (~7 min) than that of adult muscle AChRs expressed in CHO-K1/A5 cells[34] (~5.0 h), BC3H-1 cells[34] (~7.7 h), or Q-A33 quail fibroblasts transfected with the adult AChR[35] (~9.8 h). The shorter half-life of the α7 AChRs at the cell membrane may be due to a lack of α7 AChRs at the cell membrane. Alternatively, this short half-life could be the result of a defective interaction between the α7 AChRs proteins needed for long-term receptor stability. Gu *et al*[36] suggested that the metabolic stability of the AChR arises from its association with other proteins that

825

stabilize it, which are presumably absent from SHE-P1 cells. In our experiment, the dissociation constant K_D for αBTX binding to the α7 AChR was rather high compared to previously published values[37, 38]. However, it was in agreement with the very short incubation times used in the radioligand and fluorescent binding assays. In addition, incubations with fluorescent αBTX for periods longer than 15 minutes resulted in the internalization of α7 AChRs (see Figure 3, supplementary material). Furthermore, stably expressed α7 AChRs exhibited *in vitro* pharmacological properties typical of this type of AChR. Inhibition of $[I^{125}]$αBTX binding by nicotine displayed an IC_{50} of ~40 nmol/L, in agreement with previous reports for mammalian cells in culture[39]. The calculated value for the K_i was also similar to that which was previously reported[37].

As for the ion permeation properties of the stably expressed α7 AChR in the new SHE-P1-hα7-Ric-3 cell line, patch-clamp recordings showed single-channel currents when exposed to the natural agonist ACh. The observed kinetic parameters are compatible with those reported for α7 AChRs transiently expressed in oocytes[19] and in BOSC 23 cells[20]. A recent report[21] describing the functional properties of α7 AChRs heterologously expressed in CHO cells failed to observe receptor-mediated Ca^{2+} fluxes when nicotinic agonists were used to activate the AChR in the absence of the positive allosteric modulator PNU-120596 or after pretreatment of cells with the tyrosine kinase inhibitor genistein.

The production of a stable cell line that expresses high levels of cell-surface receptors and exhibits channel activation with the natural agonist acetylcholine, as reported here, constitutes an important advancement in the study of neuronal α7-type homomeric receptors in mammalian cells.

Acknowledgements

Author contribution

Francisco J BARRANTES and A Sofía VALLÉS designed the research; A Sofía VALLÉS and Ana M ROCCAMO performed the research; A Sofía VALLÉS analyzed the data; Francisco J BARRANTES and A Sofía VALLÉS wrote the paper.

References

1 Millar NS, Harkness PC. Assembly and trafficking of nicotinic acetylcholine receptors (Review). Mol Membr Biol 2008; 25: 279–92.

2 Lester HA, Dibas MI, Dahan DS, Leite JF, Dougherty DA. Cys-loop receptors: new twists and turns. Trends Neurosci 2004; 27: 329–36.

3 Role LW, Berg DK. Nicotinic receptors in the development and modulation of CNS synapses. Neuron 1996; 16: 1077–85.

4 Jones S, Sudweeks S, Yakel JL. Nicotinic receptors in the brain: correlating physiology with function. Trends Neurosci 1999; 22: 555–6.

5 Seguela P, Wadiche J, Neley-Miller K, Dani JA, Patrick JW. Molecular cloning, functional properties, and distribution of rat brain alpha 7: a nicotinic cation channel highly permeable to calcium. J Neurosci 1993; 13: 596–604.

6 Gotti C, Clementi F. Neuronal nicotinic receptors: from structure to pathology. Prog Neurobiol 2004; 74: 363–96.

7 Puchacz E, Buisson B, Bertrand D, Lukas RJ. Functional expression of nicotinic acetylcholine receptors containing rat alpha 7 subunits in human SH-SY5Y neuroblastoma cells. FEBS Lett 1994; 354: 155–9.

8 Zhao L, Kuo YP, George AA, Peng JH, Purandare MS, Schroeder KM, *et al*. Functional properties of homomeric, human alpha 7-nicotinic acetylcholine receptors heterologously expressed in the SH-EP1 human epithelial cell line. J Pharmacol Exp Ther 2003; 305: 1132–41.

9 Cooper ST, Millar NS. Host cell-specific folding of the neuronal nicotinic receptor alpha8 subunit. J Neurochem 1998; 70: 2585–93.

10 Cooper ST, Millar NS. Host cell-specific folding and assembly of the neuronal nicotinic acetylcholine receptor alpha7 subunit. J Neurochem 1997; 68: 2140–51.

11 Kassner PD, Berg DK. Differences in the fate of neuronal acetylcholine receptor protein expressed in neurons and stably transfected cells. J Neurobiol 1997; 33: 968–82.

12 Rangwala F, Drisdel RC, Rakhilin S, Ko E, Atluri P, Harkins AB, *et al*. Neuronal alpha-bungarotoxin receptors differ structurally from other nicotinic acetylcholine receptors. J Neurosci 1997; 17: 8201–12.

13 Williams ME, Burton B, Urrutia A, Shcherbatko A, Chavez-Noriega LE, Cohen CJ, *et al*. Ric-3 promotes functional expression of the nicotinic acetylcholine receptor alpha7 subunit in mammalian cells. J Biol Chem 2005; 280: 1257–63.

14 Castillo M, Mulet J, Gutierrez LM, Ortiz JA, Cautelan F, Gerber S, *et al*. Dual role of the RIC-3 protein in trafficking of serotonin and nicotinic acetylcholine receptors. J Biol Chem 2005; 280: 27062–8.

15 Drisdel RC, Manzana E, Green WN. The role of palmitoylation in functional expression of nicotinic alpha7 receptors. J Neurosci 2004; 24: 10502–10.

16 Lansdell SJ, Gee VJ, Harkness PC, Doward AI, Baker ER, Gibb AJ, *et al*. RIC-3 enhances functional expression of multiple nicotinic acetylcholine receptor subtypes in mammalian cells. Mol Pharmacol 2005; 68: 1431–8.

17 Lansdell SJ, Collins T, Yabe A, Gee VJ, Gibb AJ, Millar NS. Host-cell specific effects of the nicotinic acetylcholine receptor chaperone RIC-3 revealed by a comparison of human and Drosophila RIC-3 homologues. J Neurochem 2008; 105: 1573–81.

18 Palma E, Maggi L, Barabino B, Eusebi F, Ballivet M. Nicotinic acetylcholine receptors assembled from the alpha7 and beta3 subunits. J Biol Chem 1999; 274: 18335–40.

19 Fucile S, Palma E, Martinez-Torres A, Miledi R, Eusebi F. The single-channel properties of human acetylcholine alpha 7 receptors are altered by fusing alpha 7 to the green fluorescent protein. Proc Natl Acad Sci U S A 2002; 99: 3956–61.

20 Bouzat C, Bartos M, Corradi J, Sine SM. The interface between extracellular and transmembrane domains of homomeric Cys-loop receptors governs open-channel lifetime and rate of desensitization. J Neurosci 2008; 28: 7808–19.

21 Roncarati R, Seredenina T, Jow B, Jow F, Papini S, Kramer A, *et al*. Functional properties of alpha7 nicotinic acetylcholine receptors co-expressed with RIC-3 in a stable recombinant CHO-K1 cell line. Assay Drug Dev Technol 2008; 6: 181–93

22 Peng JH, Lucero L, Fryer J, Herl J, Leonard SS, Lukas RJ. Inducible, heterologous expression of human alpha7-nicotinic acetylcholine receptors in a native nicotinic receptor-null human clonal line. Brain Res 1999; 825: 172–9.

23 Cheng Y, Prusoff WH. Relationship between the inhibition constant (K1) and the concentration of inhibitor which causes 50 per cent inhibition (I50) of an enzymatic reaction. Biochem Pharmacol 1973; 22: 3099–08.

24 Ross RA, Spengler BA, Biedler JL. Coordinate morphological and biochemical interconversion of human neuroblastoma cells. J Natl Cancer Inst 1983; 71: 741–7.

25 Barrantes FJ. Cholesterol effects on nicotinic acetylcholine receptor. J Neurochem 2007; 103: 72–80.

26 Yamanaka K, Kigoshi S, Muramatsu I. Muscarinic receptor subtypes in bovine adrenal medulla. Biochem Pharmacol 1986; 35: 3151–7.

27 Couturier S, Bertrand D, Matter JM, Hernandez MC, Bertrand S, Millar N, *et al*. A neuronal nicotinic acetylcholine receptor subunit (alpha 7) is developmentally regulated and forms a homo-oligomeric channel blocked by alpha-BTX. Neuron 1990; 5: 847–56.

28 Gerzanich V, Anand R, Lindstrom J. Homomers of alpha 8 and alpha 7 subunits of nicotinic receptors exhibit similar channel but contrasting binding site properties. Mol Pharmacol 1994; 45: 212–20.

29 Gotti C, Hanke W, Maury K, Moretti M, Ballivet M, Clementi F, *et al*. Pharmacology and biophysical properties of alpha 7 and alpha 7-alpha 8 alpha-bungarotoxin receptor subtypes immunopurified from the chick optic lobe. Eur J Neurosci 1994; 6: 1281–91.

30 Cooper ST, Millar NS. Host cell-specific folding of the neuronal nicotinic receptor alpha8 subunit. J Neurochem 1998; 70: 2585–93.

31 Green WN, Millar NS. Ion-channel assembly. Trends Neurosci 1995; 18: 280–7.

32 Baier CJ, Barrantes FJ. Sphingolipids are necessary for nicotinic acetylcholine receptor export in the early secretory pathway. J Neurochem 2007; 101: 1072–84.

33 Pediconi MF, Gallegos CE, De Los Santos EB, Barrantes FJ. Metabolic cholesterol depletion hinders cell-surface trafficking of the nicotinic acetylcholine receptor. Neuroscience 2004; 128: 239–49.

34 Roccamo AM, Pediconi MF, Aztiria E, Zanello L, Wolstenholme A, Barrantes FJ. Cells defective in sphingolipids biosynthesis express low amounts of muscle nicotinic acetylcholine receptor. Eur J Neurosci 1999; 11: 1615–23.

35 Kopta C, Steinbach JH. Comparison of mammalian adult and fetal nicotinic acetylcholine receptors stably expressed in fibroblasts. J Neurosci 1994; 14: 3922–33.

36 Gu Y, Franco A Jr, Gardner PD, Lansman JB, Forsayeth JR, Hall ZW. Properties of embryonic and adult muscle acetylcholine receptors transiently expressed in COS cells. Neuron 1990; 5: 147–57.

37 Gopalakrishnan M, Buisson B, Touma E, GiordanoT, Campbell JE, Hu IC, *et al*. Stable expression and pharmacological properties of the human alpha 7 nicotinic acetylcholine receptor. Eur J Pharmacol 1995; 290: 237–46.

38 Anand R, Peng X, Lindstrom J. Homomeric and native alpha 7 acetylcholine receptors exhibit remarkably similar but non-identical pharmacological properties, suggesting that the native receptor is a heteromeric protein complex. FEBS Lett 1993; 327: 241–6.

39 Peng X, Katz M, Gerzanich V, Anand R, Lindstrom J. Human alpha 7 acetylcholine receptor: cloning of the alpha 7 subunit from the SH-SY5Y cell line and determination of pharmacological properties of native receptors and functional alpha 7 homomers expressed in Xenopus oocytes. Mol Pharmacol 1994; 45: 546–54.